

Single-strand recombination signal sequence nicks *in vivo*: evidence for a capture model of synapsis

John D Curry, Jamie K Geier & Mark S Schlissel

Variable (diversity) joining (V(D)J) recombination is initiated by the introduction of single-strand DNA breaks (nicks) at recombination signal sequences (RSSs). The importance and fate of these RSS nicks for the regulation of the V(D)J rearrangement and their potential contribution to genomic instability are poorly understood. Using two new methodologies, we were able to detect and quantify specific RSS nicks introduced into genomic DNA by incubation with recombination-activating gene proteins *in vitro*. *In vivo*, however, we found that nicks mediated by recombination-activating gene (RAG) proteins were detectable only in gene segments associated with RSSs containing 12-base pair spacers but not in those containing 23-base pair spacers. These data support a model of capture rather than synapsis for pairwise RSS cleavage during V(D)J recombination.

Immune-receptor diversity is dependent on a unique, lymphoid-restricted set of site-specific DNA recombination reactions known as variable (diversity) joining (V(D)J) recombination^{1,2}. Recombination of immunoglobulin and T cell receptor (TCR) gene segments is catalyzed in part by products of the recombination-activating gene 1 (*Rag1*) and *Rag2* (refs. 3,4). These rearranging gene segments are flanked by well conserved recombination signal sequences (RSSs)². An RSS consists of a dyad-symmetric heptamer (5'-CACAGTG-3') followed by either 12 ± 1 bases (RSS-12) or 23 ± 1 bases (RSS-23) of poorly conserved sequence and an A-T-rich nonamer (5'-ACAAAACC-3'). Only gene segments flanked by dissimilar RSS-12 and RSS-23 sequences are permitted to recombine, a restriction known as the '12/23 rule'². *In vitro* studies have shown that a heteromultimer of RAG proteins binds to a pair of RSSs⁵. The RAG complex then introduces single-strand nicks precisely at the junctions between the RSSs and coding segments, leaving a 3'-hydroxyl group on each coding end⁶. These 3'-hydroxyl groups are then activated to attack the opposite phosphodiester bonds, cleaving the DNA and forming hairpin loops on the coding ends and blunt 5'-phosphorylated double-strand breaks on the signal ends⁷⁻¹⁰. The hairpin ends are opened through the cooperative action of DNA-dependent protein kinase (DNA-PK) and Artemis (an endonuclease), are processed and then finally are joined by the promiscuously expressed nonhomologous end-joining (NHEJ) machinery to form a coding joint⁵. The blunt-ended RSS fragments are also joined, forming a reaction byproduct known as a signal joint¹¹.

RAG proteins can bind, nick and then cleave RSS-containing DNA *in vitro*⁶. In the presence of Mn²⁺, the RAG proteins generate precise double-strand DNA (dsDNA) breaks on individual RSS-12 or RSS-23 substrates. In a Mg²⁺ buffer, however, the presence of both

RSS-12 and RSS-23 substrates is required for double-stranded cleavage¹². Notably, in the presence of Mg²⁺, the RAG proteins will nick individual RSS-12 or RSS-23 substrates in the absence of their complementary RSS partner¹². That last observation emphasizes the possibility that RAG protein complexes may bind and nick many individual RSSs *in vivo* with dsDNA breakage occurring only after RSS-12-to-RSS-23 synapsis.

Whereas *ex vivo* studies have reported on the characterization of coding and signal joints¹³ and then later of signal and coding ends^{9,10,14}, little is known about the formation and stability of the initial DNA nicks *in vivo*. A variety of issues concerning the timing, regulation and persistence of V(D)J recombinase-mediated DNA nicks remain unresolved. Do the RAG proteins bind to and nick many RSS elements before the synapsis and cleavage of a particular pair of RSSs? Are RAG-mediated RSS nicks involved in regulating the recombination machinery? Do these single-strand breaks persist or are they immediately converted to dsDNA breaks *in vivo*? These questions are of particular importance given the report that such nicks are highly recombinogenic and may cause genomic instability^{15,16}.

Biochemical data have led to the suggestion that RAG protein complexes may preferentially assemble on one RSS (perhaps the RSS-12, which data suggest has a higher affinity for RAG protein complexes when associated with a nucleosome¹⁷) and then capture the second RSS as free DNA¹⁸. This is in contrast to a model in which RAG protein complexes form on both RSSs and then synapse through protein-protein interaction before dsDNA breakage. Although data in support of the 'capture' model are compelling, those experiments were done *in vitro* using large amounts of recombinant 'core-RAG' proteins. 'Core-RAG' proteins are truncation mutants of RAG1 and RAG2 that contain the minimally active domains of each protein and

Department of Molecular and Cell Biology, Division of Immunology, University of California, Berkeley, California, 94720-3200, USA. Correspondence should be addressed to M.S.S. (mss@berkeley.edu).

Received 1 August; accepted 16 September; published online 13 November 2005; doi:10.1038/ni1270

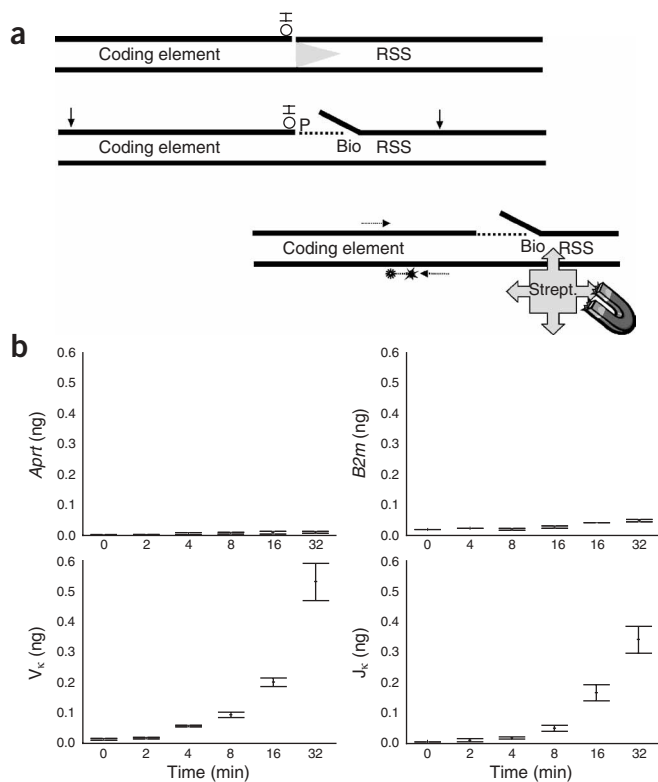


Figure 1 Oligo-capture assay for RSS nicks. (a) Assay strategy. Dotted lines indicate 5' phosphorylated (P) and 3' biotinylated (Bio) capture oligonucleotide; vertical arrows indicate restriction enzyme sites; horizontal arrows indicate PCR primers; starred line indicate the dual-labeled real-time PCR probe. Once ligated, the biotinylated capture oligonucleotide is bound to a streptavidin (Strept.)-coated paramagnetic bead and that complex is fractionated under a strong magnetic field. (b) Representative data from a typical oligo-capture assay of 63-12 genomic DNA treated *in vitro* with core-RAG1 and core-RAG2 proteins, showing the amount of recovered DNA for each target sequence as a function of the time of incubation. Data represent mean values \pm s.d. from three independent quantitative real-time PCR analyses for each DNA sample. Results are expressed in nanograms (ng) on the basis of a standard curve generated with various amounts of unfractionated genomic DNA.

We used the oligo-capture assay to measure RSS nicks associated with rearranging gene segments in pro-B cell lines and in lymphoid progenitors from mouse bone marrow and thymus. Our data suggest that RSS nicking by the V(D)J recombinase is developmentally regulated and that the recombination machinery preferentially targets RSS-12. These data suggest that RSS-23 capture may be rate limiting for recombination in accessible rearranging loci.

RESULTS

Oligo-capture assay for RAG-mediated RSS nicks

As described above, the V(D)J recombinase nicks DNA precisely at the junction between the conserved RSS heptamer and the end of an immunoglobulin or TCR coding segment. We reasoned that a short 5'-phosphorylated oligonucleotide complementary to the heptamer sequence of the intact strand might displace the nicked strand and be capable of ligation to the exposed 3'-hydroxyl group on the coding end (Fig. 1a). To test that idea, we treated purified high-molecular-weight genomic DNA from the *Rag2*^{-/-} cell line 63-12 with recombinant core-RAG1 and core-RAG2 proteins *in vitro* for various lengths of time. We then ligated a biotinylated 'capture' oligonucleotide to the RAG-treated DNA. We digested ligated DNA with restriction enzymes and magnetically fractionated it using streptavidin-conjugated paramagnetic beads. We finally quantified captured DNA using various quantitative real-time PCR assays. We compared captured DNA from two loci that lacked RSS sequences (adenine phosphoribosyltransferase (*Aprt*) and β_2 -microglobulin (*B2m*)) with that from *V κ* and *J κ* gene segments bearing RSS-12 or RSS-23 sequences, respectively (Fig. 1b). There was increasing *V κ* and *J κ* capture dependent on the length of incubation

are highly soluble. The relevance of such an RSS capture model *in vivo* has yet to be determined.

In an attempt to address these issues, we used two different methods to capture and quantify single-strand breaks in genomic DNA. The first of these methods, called the 'oligo-capture assay' here, is sequence specific and relies on the ligation of a complementary biotin-labeled oligonucleotide to the free 3'-hydroxyl group of nicked RSSs in genomic DNA. The second method involves nick translation of genomic DNA with biotin-labeled ddUTP and *Escherichia coli* DNA polymerase I¹⁹. In both approaches, biotin-labeled genomic DNA is then restriction digested and fractionated using streptavidin-coated paramagnetic beads, and captured DNA is analyzed by quantitative real-time PCR assay.

Figure 2 Limit of detection and specificity of the oligo-capture assay. (a) Oligo-capture assay with genomic DNA treated with the nicking endonuclease N.Alw I. Various percentage mixtures of N.Alw I-nicked and untreated 63-12 genomic DNA were subjected to oligo-capture with a specific heptamer oligonucleotide homologous to DNA adjacent to an N.Alw I nick site near the DFL16.1 *Igh* gene segment. Far right, capture with a nonspecific oligonucleotide (the pCACAGTG-biotin oligonucleotide used in Fig. 1). (b) Effect of oligonucleotide sequence on capture assay results. Biotin-labeled oligonucleotides (horizontal axis) were used to capture nicked *V κ* RSS-12 sequences (1, 3, 5 and 7) in genomic DNA purified from 103/BclX7 cells induced to recombine their κ loci by growth at the restrictive temperature. Oligonucleotides pCACAGTG, pCACAGAA and pCACAATG are variations on the RSS heptamer consensus sequence, whereas pTCGACGA is a randomized sequence with a base composition identical to that of the consensus sequence. Data are representative; for each point the mean \pm s.d. from three independent quantitative real-time PCR analyses is presented.

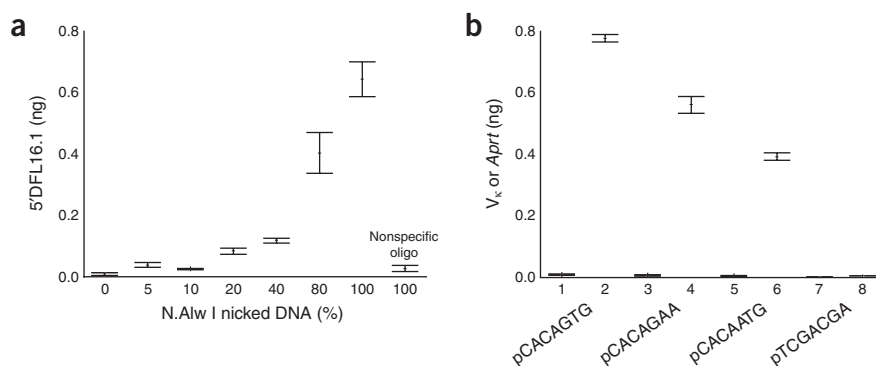


Figure 3 DNA nicks at V_{κ} RSS-12 but not J_{κ} RSS-23 sequences in pro-B cell lines induced to rearrange the *Igk* locus. **(a,b)** 103/BclX7 **(a)** and E2A **(b)** were induced to activate *Igk* rearrangement by either temperature shift or STI-571 treatment, respectively. DNA was purified after various lengths of time and analyzed by oligo capture for nicks in *B2m*, J_{κ} RSS-23 or V_{κ} RSS-12 sequences. $V_{\kappa}220$ quantitative real-time PCR **(a, bottom)** detects only 4 of the 40 V_{κ} gene segments detected in the V_{κ} assay **(a, V_{κ})**. 103/BclX7 **(b)**, sample of 103/BclX7 cultured at the restrictive temperature for 20 h (positive control). Data are representative data; for each point the mean \pm s.d. from three independent quantitative real-time PCR analyses is presented. **(c)** Detection of dsDNA breaks and V_{κ} -to- J_{κ} coding joints in genomic DNA. Genomic DNA samples from the 24-hour time points in **a** and **b** were analyzed by ligation-mediated PCR for dsDNA RSS breaks at $J_{\kappa}1$ (top) and $V_{\kappa}4$ (middle). The same DNAs were also assayed for V_{κ} -to- J_{κ} coding joints (bottom). 63-12, DNA from a *Rag2*^{-/-} pro-B cell line; M, molecular weight marker. Data represent digital images of ethidium bromide-stained gels of PCR products.

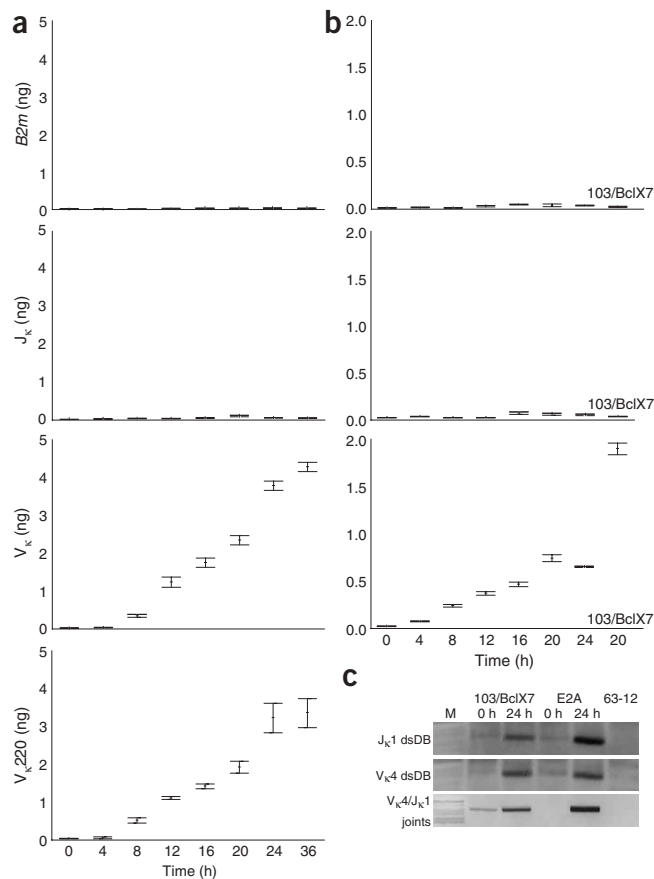
with RAG proteins, whereas the amounts of *Aprt* and *B2m* recovered remained constant. We obtained the same results with other immunoglobulin and TCR gene segments (**Supplementary Fig. 1** online). In addition, we found that this oligo-capture assay did not detect dsDNA breaks at RSSs or other DNA sequences (data not shown).

To determine the sensitivity and specificity of the oligo-capture assay, we treated high-molecular-weight 63-12 genomic DNA with the restriction enzyme N.Alw I, which introduces a single-stranded DNA (ssDNA) nick adjacent to its target site. We then mixed the digested DNA at various ratios with untreated genomic DNA and carried out the oligo-capture assay using a 7-nucleotide capture oligonucleotide complementary to sequences immediately adjacent to an N.AlwI nick site near the DFL16.1 immunoglobulin heavy-chain (*Igh*) D segment. As the fraction of nicked DNA increased from 0 to 100%, the amount of recovered DFL16.1 fragments increased as well (**Fig. 2a**). When we ligated an oligonucleotide used before for the capture of nicked RSS heptamers, however, no DFL16.1 fragments were captured.

To further test the specificity of the capture assay, we used DNA purified from a pro-B cell line (103/BclX7) transformed with a temperature-sensitive Abelson murine leukemia virus (A-MuLV) that induces high frequencies of *Igk* locus rearrangement when grown in nonpermissive conditions²⁰. We ligated genomic DNA purified from 103/BclX7 cells grown in inducing conditions to each of three capture oligonucleotides that matched or varied by one or two nucleotides from the consensus RSS-heptamer and to a fourth capture oligonucleotide that was completely divergent. The most V_{κ} DNA was captured using the heptamer consensus oligonucleotide (**Fig. 2b**, lane 2). Use of the minimally divergent capture oligonucleotides resulted in intermediate recovery of V_{κ} DNA, whereas the fully divergent oligonucleotide (**Fig. 2**, lane 8) captured only background amounts of V_{κ} DNA. None of the four oligonucleotides captured non-RSS-bearing *Aprt* sequences (**Fig. 2b**, lanes 1, 3, 5 and 7). In addition, DNA breaks introduced by apoptosis-associated nucleases had a minimal effect on the oligo-capture assay (**Supplementary Fig. 2** online).

Nicked RSS-12 accumulate at rearranging loci *in vivo*

The single-strand nicking and double-strand breakage steps of V(D)J recombination can be unlinked from one another *in vitro*¹². To determine whether specific RSS nicks exist *in vivo* in cells undergoing V(D)J recombination, we tested DNA purified from two A-MuLV-transformed mouse pro-B cell lines induced to activate the V(D)J recombinase. The first was the temperature-inducible 103/BclX7 line mentioned earlier. The second, E2A, is a cell line transformed with wild-type A-MuLV²¹ that can be induced to undergo *Igk* rearrangement by treatment with the Abl kinase inhibitor STI-571 (ref. 22). We

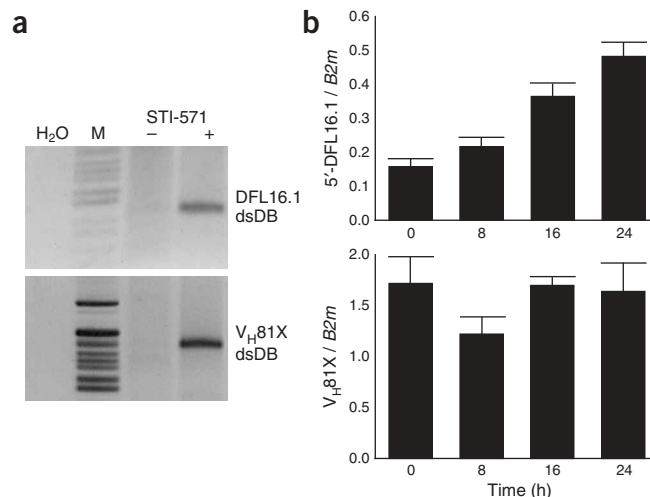


purified genomic DNA from each cell line after culture for various lengths of time in inducing conditions. We then assayed the DNA for nicks at V_{κ} RSS-12s and J_{κ} RSS-23s as well as in the control *B2m* gene. In both sets of samples, we detected increasing amounts of nicked V_{κ} RSS-12 but not J_{κ} RSS-23 or *B2m* DNA, starting within 8 h of the start of STI-571 treatment and increasing throughout the culture period (**Fig. 3a,b**).

The quantitative real-time PCR assay for V_{κ} sequences used in these experiments relies on modestly degenerate oligonucleotides that have the potential to detect approximately 40 V_{κ} gene segments, whereas the J_{κ} assay detects only 4 J_{κ} gene segments. Each assay, however, is quantified on the basis of a standard curve created using total genomic DNA. To eliminate the possibility of misleading results arising from the disparate number of gene segments detected in the two assays, we devised an alternative set of V_{κ} primers ($V_{\kappa}220$) that detect only four V_{κ} gene segments. Using these more selective quantitative real-time PCR primers, we noted the same time-dependent increase in V_{κ} nicks in the temperature-sensitive cell line (**Fig. 3a**, bottom). In contrast to the presence of nicks on V_{κ} but not J_{κ} RSSs, we were able to detect dsDNA breaks at both V_{κ} and J_{κ} RSSs in these same samples using ligation-mediated PCR⁹ (**Fig. 3c**). In addition, V_{κ} -to- J_{κ} coding joints were detectable after 24 h of induction in both cell lines (**Fig. 3c**). These data suggest that the formation of RAG-dependent RSS-12 nicks is the first step in V(D)J recombination and is followed by RSS-23 capture, dsDNA breakage and coding-joint formation.

E2A cells contain two DJ-rearranged *Igh* alleles (DFL16.1- $J_{H}3$ and DSP2.9- $J_{H}1$; data not shown). As a result, we were able to assay for ssDNA nicks and dsDNA breaks associated with V_{H} RSS-23 and D_{H}

Figure 4 DNA nicks and breaks in the *Igh* locus. (a) Ligation-mediated PCR assay of dsDNA RSS breaks at D_H and V_H RSSs. Genomic DNA purified from untreated (-) and STI-571-treated (+) E2A cultures was assayed for dsDNA breaks 5' of the DFL16.1 D_H gene segment (top) and 3' of the V_H 81X gene segment (bottom). H₂O, control lacking template; M, molecular weight marker. Data represent digital images of ethidium bromide-stained agarose gels. (b) DNA nicks at the DFL16.1 gene segment. E2A cells were induced for various lengths of time by culture in the presence of STI-571. Genomic DNA was purified and assayed by oligo capture for DFL16.1 RSS-12 (upper) and V_H 81X RSS-23 (lower) nicks. RSS target values were divided by *Aprt* control values to correct for the effects of background labeling of adventitious DNA nicks. Data are representative data; for each point the mean \pm s.d. from three independent quantitative real-time PCR analyses is presented.



RSS-12 gene segments in DNA from cultures treated with STI-571. The treated cells showed a substantial increase in dsDNA RSS signal breaks at the RSS-23 3' of V_H 81X (the most D-proximal and frequently rearranged V_H gene segment) and at the RSS-12 5' of DFL16.1 (the most 5' D_H gene segment) (Fig. 4a). As with the *Igk* locus, however, treated cells showed a time-dependent increase in RSS-12 (DFL16.1) but not RSS-23 (V_H 81X) ssDNA RSS nicks (Fig. 4b).

We were unsuccessful in several attempts to detect V_K or J_K nicks in highly purified primary bone marrow progenitor B cell DNA (data not shown). That may have been a result of the low frequency of actively rearranging alleles in primary pre-B cells²³. We were, however, able to detect *Tcra* locus nicks in thymocytes from young mice. Using the oligo-capture assay, we detected RAG-dependent nicks at the TCR $J_{\alpha}50$ RSS-12 but not at the TCR $V_{\alpha}13$ RSS-23 in genomic DNA from thymocytes at day 8 and 15 compared with negative control RAG1-deficient TCR $\alpha\beta$ transgenic mouse thymocyte DNA (Fig. 5). Of the nine members of the $V_{\alpha}13$ gene-segment family, the quantitative real-time PCR assay was able to detect six (data not shown).

An alternative assay shows nicking of RSS-12 sequences

We developed a second method to confirm the results of the oligo-capture assay. We used a traditional nick-translation assay with *E. coli* DNA polymerase I to introduce a single biotin-labeled dideoxy-UTP (ddUTP) residue into DNA 3' to a nick (Fig. 6a). Although this strategy ensures that a single biotin label is incorporated 3' to nicks in genomic DNA, this biotin labeling is not specific for RSS nicks. Nonspecific labeling in this system was extremely high, as random nicks and some 5' overhanging dsDNA breaks could also be labeled. To minimize background resulting from mechanical shearing, we prepared genomic DNA by embedding cells in agarose plugs and did the modified nick-translation assay in the plugs. To detect V_K RSS

nicks above background, we divided the target V_K signal by the quantitative real-time PCR signal from the nontarget control locus, *Aprt*. Using this alternative approach, we were able to detect nicks at V_K gene segments in induced 103/BclX7 cells that increased steadily with time (Fig. 6). Again, nicks at the J_K gene segments could not be detected above the background. The 49-hour sample showed a substantially decreased signal, which was likely to have been caused by the deteriorated condition of the cells at this much later time point. These results provide an independent confirmation of observations made using the oligo-capture assay: nicks can be detected at RSS-12 but not RSS-23 sequences at loci undergoing V(D)J recombination.

RAG proteins are associated with V_K RSSs *in vivo*

Our ability to detect nicked V_K RSS-12 sequences led us to consider whether these nicked RSSs might remain associated with RAG1 and RAG2 protein complexes *in vivo*, awaiting RSS-23 capture before proceeding to dsDNA cleavage. To address that issue, we carried out chromatin immunoprecipitation of uninduced and induced 103/BclX7 cells using antisera to RAG2 or to acetylated histone H3. In each of two independent experiments, we found that the ratio of V_K to J_K sequences in the RAG2 chromatin immunoprecipitations increased after induction of recombination (Fig. 6d). In contrast, this ratio remained unchanged in the acetylated histone H3 chromatin immunoprecipitations (Fig. 6e). Thus, it seems that V_K RSS-12 sequences may remain complexed with RAG proteins after nicking.

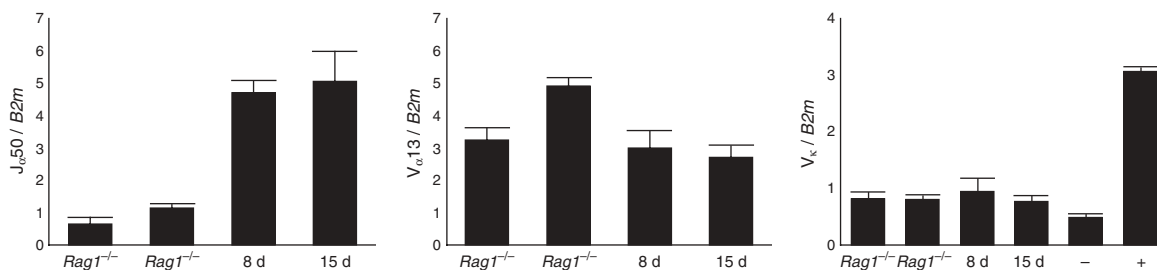


Figure 5 DNA nicks at $J_{\alpha}50$ RSS-12 but not $V_{\alpha}13$ RSS-23 or V_K RSS-12 sequences in thymocyte genomic DNA. Oligo-capture assays were done on DNA purified from thymocytes taken from two different *Rag1*^{-/-} $\alpha\beta$ TCR-transgenic mice and from wild-type nontransgenic mice 8 and 15 d of age. The captured DNA was analyzed for $J_{\alpha}50$ (left), $V_{\alpha}13$ (middle) and V_K (right) sequences. 63-12 genomic DNA incubated in the presence (+) or absence (-) of core-RAG1 and core-RAG2 proteins served as controls for the V_K assays. Each assay was normalized by the nonspecific capture of *B2m* DNA. Data are representative data; for each point the mean \pm s.d. from three independent quantitative real-time PCR analyses is presented.

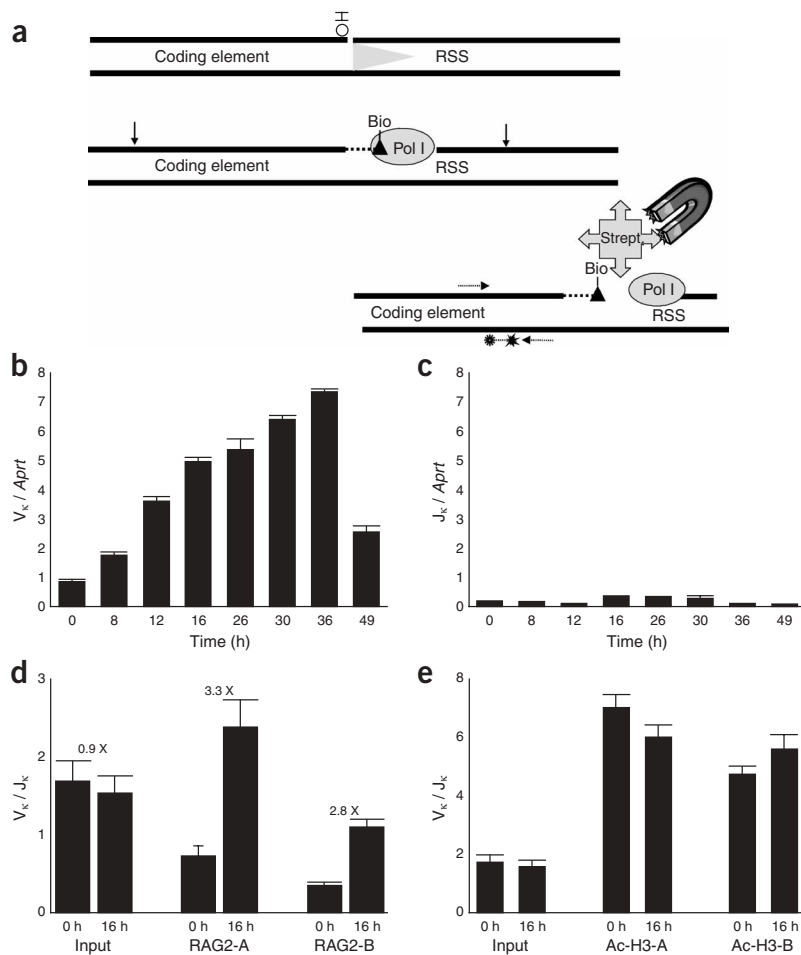


Figure 6 Alternative assays for RAG1 and RAG2 activity on RSS-12 and RSS-23 DNA. **(a)** Nick-translation strategy for the labeling and capture of nicked RSS DNA. Chain-terminating and biotinylated ddUTP (filled triangles) is incorporated downstream of the 3'-hydroxyl groups on nicked DNA with DNA polymerase I. Restriction enzymes (vertical arrows indicate sites) are used to fragment the labeled high-molecular-weight DNA. Streptavidin-coated paramagnetic beads (Strept.) capture the biotin-labeled DNA fragments, which are then separated from unlabeled DNA fragments by a strong magnetic field. Horizontal arrows indicate the positions of quantitative real-time PCR primers; starred line indicates the hydrolysis probe used for real-time PCR quantification. **(b,c)** Quantitative real-time PCR assays of captured V_{κ} RSS-12 and J_{κ} RSS-23 sequences. DNA was purified from 103/BcIX7 cells cultured at the nonpermissive temperature (time, horizontal axes) and subjected to nick-translation assay for DNA nicks. Target gene results were divided by the results of the control gene *Aprt*. **(d,e)** Chromatin immunoprecipitation assays. Sonicated, fixed chromatin from 103/BcIX7 cells cultured at the permissive (0 h) or nonpermissive temperature (16 h) was subjected to chromatin immunoprecipitation with antibody to RAG2 (**d**) or to acetylated histone H3 (Ac-H3; **e**). Precipitated DNA was recovered and was analyzed by quantitative real-time PCR for V_{κ} and J_{κ} DNA sequences; ratios of these are shown. -A and -B, two independent experiments; numbers above s.d. bars in **d** indicate the relative difference in the V_{κ}/J_{κ} ratio for uninduced versus induced cell DNA. Data are representative of the mean \pm s.d. from three independent quantitative real-time PCR analyses.

Recombinase nicking is developmentally regulated

The V(D)J recombinase generates dsDNA RSS breaks in a developmentally regulated way²⁴. We used the oligo-capture assay to determine whether RSS nicking was likewise regulated. We considered it possible that at some loci V(D)J recombination might be regulated at the level of synapsis (locus compaction) or dsDNA cleavage rather than at the level of RSS binding or DNA nicking. To test that idea, we assayed for V_{κ} RSS-12 nicks in the same thymocyte genomic DNA in which $J_{\gamma}50$ RSS-12 nicks had been detected before. We were unable to detect any V_{κ} nicks in DNA from young mouse thymocytes above the low background signal seen in *Rag1*^{-/-} TCR $\alpha\beta$ -transgenic thymocyte DNA (**Fig. 5**). Thus we conclude that *Igk* loci RSSs seem inaccessible to RAG1 and RAG2 protein binding in thymocytes.

DISCUSSION

Studies of the regulation of the V(D)J recombinase in lymphoid cells have relied on assays for dsDNA RSS breaks or complete coding joints^{9,10,14,25}. Here we have extended the ability to analyze recombinase activity back to the first catalytic step in the reaction pathway, the generation of sequence-specific ssDNA nicks at RSSs. We found that many rearranging gene segments with RSS-12 signals contained a precisely positioned nick at the RSS-coding segment junction, whereas potential rearranging partners with RSS-23 signals were mostly intact. These data support a capture model of recombination in which the RAG proteins first form a complex on an RSS-12 and then capture an RSS-23 as free DNA, rather than a synapsis model in which RAG

proteins bind and nick both RSS types and then require association of RAG-RSS complexes to complete the recombination reaction¹⁸.

The capture model for V(D)J recombination was initially proposed based on biochemical experiments using RSS-containing oligonucleotides and recombinant core-RAG proteins¹⁸. Short double-stranded oligonucleotides bearing RSS-12 or RSS-23 sequences were mixed with recombinant core-RAG proteins in conditions that permit RSS binding but not nicking or cleavage. When preformed RSS-12 core-RAG complexes were mixed with free RSS-23 DNA in the presence of Mg^{2+} (which permits the cleavage reaction to proceed), efficient hairpin DNA formation was noted. When preformed RSS-12 core-RAG and RSS-23 core-RAG complexes were similarly mixed, the formation of RSS-12 hairpins was reduced considerably, resulting in the suggestion that the favored pathway for recombination involves formation of a RAG complex on one RSS followed by the capture of the other RSS as free DNA before subsequent cleavage. It is possible, however, that RAG-RSS complexes formed *in vitro* in the setting of high stoichiometries of core-RAG–maltose-binding protein fusion proteins (with the maltose-binding protein domain added to enhance solubility and aid in purification) used in those experiments might act differently from wild-type RAG proteins acting on a chromatinized genomic DNA substrate *in vivo*.

The strength of the data that we have presented here is that we assayed the location and activity of RAG proteins in a cellular context. The RAG proteins were full-length native proteins expressed in amounts that cells would normally maintain while attempting

recombination. In addition, the RSS targets were recognized in the context of intact chromatin structure. In cell lines in which V_{κ} -to- J_{κ} rearrangement is inducible either by temperature shift or drug treatment, we noted a time-dependent accumulation of V_{κ} RSS-12 but not J_{κ} RSS-23 signal nicks. In addition, the drug-treated cell line showed nicks at DFL16.1 RSS-12 but not V_{H} RSS-23 gene segments. Notably, dsDNA RSS breaks were common to both types of RSS, as was the formation of complete coding joints. In addition, using a chromatin immunoprecipitation assay with antibody to RAG2, we noted enrichment of V_{κ} relative to J_{κ} DNA sequences, consistent with the presence of RAG-RSS complexes on RSS-12 but not RSS-23 signals in the *Igk* locus. We made similar observations in primary thymocytes, detecting nicks at J_{α} RSS-12 but not V_{α} RSS-23.

As RSS binding by RAG proteins in appropriate conditions results in rapid nicking, it is perhaps unexpected that we did not note any RSS-23 nicking, as the RAG1 and RAG2-RSS12 complex captures the RSS-23 and goes on to effect pairwise cleavage. We suggest that RSS-23 nicking is immediately followed by nucleophilic attack (direct transesterification) resulting in the formation of dsDNA breaks, and thus the RSS-23 nicks exist only transiently in the capture complex. The nick assays presented may not be sensitive enough to detect these transient events above the 'background noise' of the assay.

The presence of dsDNA RSS breaks is a sensitive measure of the developmentally regulated pattern of V(D)J recombinase activity²⁴. For example, $J_{\kappa}1$ RSS breaks have been detected in pre-B cells but not pro-B cells or thymocytes purified from mice. The presence of these breaks also correlates with the pattern of expression of germline transcripts from actively rearranging gene segments. *In vitro* studies, however, have shown that RAG proteins can bind to RSSs, and nick them, but cannot generate dsDNA breaks in the absence of RSS-12-to-RSS-23 gene-segment pairing¹². Thus, it is possible that in some circumstances, dsDNA breakage and subsequent gene-segment joining may be regulated by the ability of RAG1-RAG2-RSS-12 and RAG2-RSS-12 complexes to capture an RSS-23, rather than by the accessibility of individual RSSs in chromatin structure. Specific impediments may exist that block the interaction of distantly separated V_{κ} and J_{κ} segments in chromatin structure, for example. Such events might also occur in the complex TCR $\alpha\delta$ locus, where an insulator sequence might contribute to the regulation of V(D)J recombination²⁶. The oligonucleotide capture assay described in this report is capable of detecting specific RSS-12 nicks that might occur without subsequent RSS-23 capture and pairwise dsDNA breakage.

In developing thymocytes, in which recombinase activity is very high and in which we readily detected RSS-12 nicks at the TCR $J_{\alpha}50$ gene segment, we were unable to detect nicks at RSS-12 associated with V_{κ} gene segments. That observation is consistent with the hypothesis that *Igk* locus rearrangement in thymocytes is regulated at the level of RSS accessibility and RAG binding rather than at the level of gene-segment pairing. Further work will be needed to determine whether this holds true for other rearranging loci.

Given the tendency of RAG protein complexes to form first on RSS-12-containing gene segments, specific mechanisms may exist to promote the capture of appropriate RSS-23-containing partners. It is possible, for example, that promoter-enhancer interactions may be responsible for the condensation of the *Igh* locus noted in B cells undergoing V-to-DJ rearrangement and that this condensation may increase the likelihood of RSS-23 capture²⁷⁻²⁹. Published work has shown that *Igh* locus contraction is RAG independent, consistent with the idea of involvement of transcriptional regulatory or other chromatin elements in RSS-23 capture²⁷. Notably, Pax5-null mice have a

defect in the rearrangement of distal V_{H} gene segments that might be due to ineffective locus contraction and RSS-23 capture²⁸.

Our ability to detect a very robust V_{κ} nicking signal in DNA from pre-B cell lines that have been induced to undergo *Igk* rearrangement raises the possibility that the RAG proteins bind to and nick many V_{κ} RSSs on each *Igk* chromosome. In the mouse genome there are 137 identified V_{κ} gene segments and only four functional J_{κ} gene segments. RAG-binding complexes at V_{κ} -RSS-12 have only a limited number of J_{κ} RSS-23 segments to capture. Therefore, it is possible that preformed RAG-RSS-12 complexes compete for J_{κ} segments to recombine with. Given the known bias of initial *Igk* rearrangement for $J_{\kappa}1$, such preformed V_{κ} -RAG complexes may enhance the rate of light-chain receptor editing on alleles with an initial autoreactive $V_{J_{\kappa}1}$ rearrangement.

Control experiments showed that the oligo-capture assay can detect a sequence-specific N.Alw I nick when the nick is present in more than 20% of the genomes included in the assay. The target of this assay is a unique genomic sequence near the DFL16.1 gene segment. The V_{κ} nick assay, in contrast, can detect nicks at approximately 40 different V_{κ} gene-segments. Both the V_{κ} and DFL16.1 real-time PCR assays used in this study were quantified relative to a total genomic DNA standard containing the full compliment of V_{κ} gene segments. Thus, the recovered V_{κ} sequences were compared with a genomic DNA standard that contained 40 PCR targets per genome; 1 ng of recovered V_{κ} sequence represents 40 times the number of targets in 1 ng of recovered N.AlwI-digested DFL16.1 sequence. Given the similar signals obtained in the V_{κ} and N.AlwI control nick assays (expressed as nanograms of recovered genomic DNA), if it is assumed that the two assays have similar efficiencies, then each *Igk*-rearranging cell may contain as many as 25-30 V_{κ} RSS-12 RAG-nicked complexes (20% of the 137 V_{κ} genes). The implications of this large number of preformed RAG complexes for the regulation of *Igk* locus rearrangement remain to be explored.

Studies have suggested that RAG-mediated DNA nicks may contribute to genomic instability^{15,16}. *Rag1* mutants that can nick but not generate dsDNA breaks at RSSs were expressed in transfected cells along with homologous recombination reporter constructs. Nicking by RAG protein complexes substantially activated homologous recombination between plasmids or between a plasmid and a chromosomal locus. Thus, the RSS-capture mechanism of gene segment pairing may not come without cost.

METHODS

Animals and cell lines. We obtained thymocytes from young wild-type and *Rag2*^{-/-} DO11.10 $\alpha\beta$ TCR-transgenic mice by conventional methods. Animal experiments adhered to protocols approved by the University of California at Berkeley Animal Care and Use Committee (R253-0405).

The tsAbl-transformed pro-B cell line 103/BclX7 (ref. 20) and the wild-type Abl-transformed pro-B cell lines E2A²¹ and 63-12 (*Rag2*-null)³⁰ were cultured in RPMI 1640 medium supplemented with 5% (volume/volume) heat-inactivated FCS, 50 μ M β -mercaptoethanol and antibiotics. V(D)J recombination was induced in 103/BclX7 cells by shifting of the cells from a permissive (33 °C) to a nonpermissive (39 °C) temperature and in E2A cells by the addition of the Abl kinase inhibitor STI-571 (1.0 μ M). Apoptotic cells were removed from cultures with Ficoll-Hypaque sedimentation before DNA extraction.

Genomic DNA preparation. We prepared genomic DNA with a modified phase-lock phenol-chloroform extraction method. Cells were lysed in detergent and the lysates were incubated with RNase A and then proteinase K before being subjected to several successive phenol-chloroform extractions and alcohol precipitation. Precipitated DNA was recovered, was washed three times in 70% ethanol, was air-dried and was resuspended in TE (10 mM Tris-HCl, pH 8.0, and 0.2 mM EDTA) and the DNA concentration was determined by

spectrophotometry. In some experiments, genomic DNA was purified from cells embedded in low-melting-point agarose with a modified version of a published technique¹⁴. The modification was an additional proteinase K treatment in a 1 mM CaCl₂ buffer after the first proteinase K incubation in 100 mM EDTA buffer.

RAG1 and RAG2 treatment of genomic DNA. Soluble 63-12 genomic DNA (250 µg) was incubated on ice with 2.7 µg copurified core-RAG1 and core-RAG2 in a buffer containing 25 mM 3-(*N*-morpholino)-propanesulfonic acid (MOPS), pH 7.0, 60 mM potassium glutamate, 10 mM KCl, 1 mM MnCl₂, 1.5 mM dithiothreitol and 250 µg of purified BSA (New England Biolabs) in a final volume of 1.2 ml. The mixture was then divided into six equal aliquots and the first reaction immediately terminated by the addition of 500 µl of stop solution (TE with 0.25% (weight/volume) SDS and 250 µg/ml proteinase K) and incubation at 56 °C for 1 h. The remaining reaction aliquots were incubated at 37 °C for various time intervals followed by an incubation with 500 µl of stop solution and processing as above. DNA was recovered by phenol-chloroform extraction and ethanol precipitation. The precipitated DNA was washed three times with 70% ethanol, were air-dried, were resuspended in TE and then were quantified by spectrophotometry.

Oligo-capture assay. Oligo-capture assays were done on purified high-molecular-weight DNA in a volume of 150 µl. Up to 15 µg of DNA was mixed with ligation buffer (Invitrogen) and 30 fmol of the biotinylated capture oligonucleotide (various heptamers; **Supplementary Table 1** online). The mixture was incubated at 14 °C for 30 min, after which 5 units of T4 DNA ligase (Invitrogen) were added. Reactions were then incubated overnight at 14 °C and were terminated by incubation at 68 °C for 30 min. The ligated DNA was digested with restriction enzymes for at least 4 h at 37 °C in a final digestion volume of 300 µl fortified with 30 µl of a 10× buffer (50 mM Tris-HCl, pH 8.0, 50 mM MgCl₂, 5 mM DTT, 500 mM NaCl) and 20 units each of *Bam*HI, *Eco*RI, *Hind*III and *Xba*I (New England Biolabs).

Biotin-labeled DNA fragments were captured with µMACS separation columns and streptavidin-coated microbeads (Miltenyi Biotec). Columns were first equilibrated for the separation by loading of 50 µl of the equilibration buffer supplied and then 200 µl of TE (pH 8.0) supplemented with 100 mM NaCl. Paramagnetic beads (5 µl) were added to the restriction-digested DNA, followed by mixing and incubation at 25 °C for 5 min. The entire volume was loaded onto an equilibrated column (while in a strong magnetic field) and then followed by a 90-µl volume of TE plus 100 mM NaCl to rinse the reaction tube. A series of 600-µl washes (NaCl with 0.1% (wt/vol) SDS in TE) was subsequently passed through the magnetized column; 1 M, 500 mM and 100 mM NaCl (22–25 °C), then two hot (65 °C) washes of 100 and 50 mM NaCl, respectively. The final washes included two 2.5-ml volumes of TE supplemented with 0.01% (vol/vol) Tween-20. To release the captured DNA, the column was removed from the magnetic field and placed over a microcentrifuge tube, 100 µl of the final wash solution was placed into the column and the column was centrifuged to ensure all the TE and DNA were recovered.

Linker-ligation PCR. Purified genomic DNAs were assayed for double-stranded DNA signal end breaks by ligation-mediated PCR as detailed⁹ with 'hemi-nested' primers listed in **Supplementary Table 2** online.

Nick-translation labeling. Nick-translation reactions were done in gel plugs containing genomic DNA. Five gel plugs (400 µl) were placed into 400 µl buffer (50 mM Tris-HCl, pH 7.5, 6 mM MgCl₂, 20 µM each of dATP, dCTP, dGTP, 10 mM β-mercaptoethanol, 10 µg/ml of BSA) with 15 units DNA polymerase I (Invitrogen) and 2 nmol ddUTP-16-biotin (Roche). Reactions were incubated for 2 h on ice and then for 1 h at 16 °C. Plugs were then washed four times with 2 ml of ice-cold TE (pH 8.0). The reactions were placed at 75 °C for 20 min to heat inactivate any remaining DNA polymerase I, and then 40 µl of 10× digestion buffer (200 mM Tris-acetate, 500 mM potassium acetate, 100 mM magnesium acetate, 10 mM DTT, pH 7.9, at 25 °C) was added. Next, the genomic DNA was restriction digested with 100 units of *Hpy*CH4 V (New England Biolabs) and the agarose was digested with 20 units of β-agarase (New England Biolabs) at 42 °C overnight. The digested DNA was then run through nucleotide-removal spin columns as directed (Qiagen). The concentration of the purified genomic DNA was determined by spectrophotometry. Before

magnetic separation, 10 µg of DNA was adjusted to 100 mM NaCl in a final volume of 300 µl of TE.

Chromatin immunoprecipitation. Chromatin immunoprecipitation was done as reported with the following modifications³¹. The temperature-sensitive 103/BclX7 cell line was shifted to the nonpermissive temperature for 16 h and formaldehyde-cross-linked chromatin was prepared. Chromatin from approximately 6 × 10⁶ cells for each time point was incubated overnight with rotation at 4 °C with 10 µg of polyclonal rabbit antibody to acetylated H3 (Upstate Biotechnologies), 10 µg of immunoaffinity-purified polyclonal antibody to RAG2 (PharMingen) or 60 µg normal rabbit serum (Jackson ImmunoResearch). Blocked IgG-Sepharose beads (Amersham Biosciences) were prepared by rotating them for 3 h at 4 °C with 10 mg/ml of BSA and 10 mg/ml of sheared salmon sperm DNA (Invitrogen). Beads were washed three times and then resuspended with IP buffer (140 mM NaCl, 1% (vol/vol) Triton X-100, 0.1% (wt/vol) sodium deoxycholate, 100 µg/ml BSA, 100 µg/ml yeast tRNA, 1 mM PMSF). The chromatin and antibodies were added to 60 µl of the resuspended beads and followed by rotation at 4 °C for 3 h. The beads were washed, the chromatin was eluted and DNA was prepared as described³¹. DNA concentration was determined by fluorimetry and 2 ng of DNA were used per quantitative real-time PCR reaction.

Quantitative real-time PCR sequence detection. *Aprt* and *B2m* sequences were assayed to provide a measure of adventitious nicks or staggered breaks (that could be labeled by DNA polymerase I) occurring at random in genomic DNA samples. The V_κ sequences detected were in the coding region and the primers contained moderate degeneracy to detect a variety of the variable elements. Other sets of primer and probe sequences (**Supplementary Table 3** online) were designed either with Primer Express (Applied Biosystems) or manually by following guidelines from Applied Biosystems on the construction of TaqMan primers and probes.

Quantitative real-time PCR was done in a reaction volume of 25 µl with an Opticon continuous fluorescence detection thermocycler (MJ Research) as described³². Data were collected and analyzed with the software supplied by the manufacturer.

Quantitative real-time PCR standard curves constructed with 63-12 (RAG null pro-B cell) genomic DNA serially diluted from 100 ng to 10 pg per reaction were analyzed in each quantitative real-time PCR assay. Quantitative PCR values for each captured biotinylated DNA sample were expressed as ng of genomic DNA based on the appropriate standard curve. Target signals were corrected by signals obtained from the *Aprt* or *B2m* assay when required. A statistical graphics package was used to generate all the graphed data providing means with standard deviations (Statistica, Statsoft).

Note: Supplementary information is available on the Nature Immunology website.

ACKNOWLEDGMENTS

We thank E. Robey for *Rag1*^{-/-} TCRαβ-transgenic mice; Y. Zhuang (Duke University, Durham, North Carolina) for the E2A cell line; and A. Winoto and members of the Schlissel lab for comments. Supported by National Institutes of Health (AI40227 and HL48702 to M.S.S.).

COMPETING INTERESTS STATEMENT

The authors declare that they have no competing financial interests.

Published online at <http://www.nature.com/natureimmunology/>

Reprints and permissions information is available online at <http://npg.nature.com/reprintsandpermissions/>

1. Tonegawa, S., Brack, C., Hozumi, N. & Pirrotta, V. Organization of immunoglobulin genes. *Cold Spring Harb. Symp. Quant. Biol.* **42**, 921–931 (1978).
2. Tonegawa, S. Somatic generation of antibody diversity. *Nature* **302**, 575–581 (1983).
3. Schatz, D., Oettinger, M. & Baltimore, D. The V(D)J recombination activating gene, RAG-1. *Cell* **59**, 1035–1048 (1989).
4. Oettinger, M., Schatz, D., Gorka, C. & Baltimore, D. RAG-1 and RAG-2, adjacent genes that synergistically activate V(D)J recombination. *Science* **248**, 1517–1523 (1990).
5. Gellert, M. V(D)J recombination: RAG proteins, repair factors, and regulation. *Annu. Rev. Biochem.* **71**, 101–132 (2002).
6. McBlane, J. *et al.* Cleavage at a V(D)J recombination signal requires only RAG1 and RAG2 proteins and occurs in two steps. *Cell* **83**, 387–395 (1995).

7. Roth, D., Menetski, J., Nakajima, P., Bosma, M. & Gellert, M. V(D)J recombination: broken DNA molecules with covalently sealed (hairpin) coding ends in scid mouse thymocytes. *Cell* **70**, 983–991 (1992).
8. Roth, D., Nakajima, P., Menetski, J., Bosma, M. & Gellert, M.V. (D)J recombination in mouse thymocytes: double-strand breaks near T cell receptor δ rearrangement signals. *Cell* **69**, 41–53 (1992).
9. Schlissel, M., Constantinescu, A., Morrow, T., Baxter, M. & Peng, A. Double-strand signal sequence breaks in V(D)J recombination are blunt, 5'-phosphorylated, RAG-dependent, and cell cycle regulated. *Genes Dev.* **7**, 2520–2532 (1993).
10. Roth, D., Zhu, C. & Gellert, M. Characterization of broken DNA molecules associated with V(D)J recombination. *Proc. Natl. Acad. Sci. USA* **90**, 10788–10792 (1993).
11. Lewis, S., Gifford, A. & Baltimore, D. DNA elements are asymmetrically joined during the site-specific recombination of κ immunoglobulin genes. *Science* **228**, 677–685 (1985).
12. van Gent, D. *et al.* Initiation of V(D)J recombinations in a cell-free system by RAG1 and RAG2 proteins. *Curr. Top. Microbiol. Immunol.* **217**, 1–10 (1996).
13. Lewis, S. & Gellert, M. The mechanism of antigen receptor gene assembly. *Cell* **59**, 585–588 (1989).
14. Schlissel, M. Structure of nonhairpin coding-end DNA breaks in cells undergoing V(D)J recombination. *Mol. Cell. Biol.* **18**, 2029–2037 (1998).
15. Neiditch, M.B., Lee, G.S., Huye, L.E., Brandt, V.L. & Roth, D.B. The V(D)J recombinase efficiently cleaves and transposes signal joints. *Mol. Cell* **9**, 871–878 (2002).
16. Lee, G., Neiditch, M., Salus, S. & Roth, D. RAG proteins shepherd double-strand breaks to a specific pathway, suppressing error-prone repair, but RAG nicking initiates homologous recombination. *Cell* **117**, 171–184 (2004).
17. Kwon, J., Imbalzano, A.N., Matthews, A. & Oettinger, M.A. Accessibility of nucleosomal DNA to V(D)J cleavage is modulated by RSS positioning and HMG1. *Mol. Cell* **2**, 829–839 (1998).
18. Jones, J. & Gellert, M. Ordered assembly of the V(D)J synaptic complex ensures accurate recombination. *EMBO J.* **21**, 4162–4171 (2002).
19. Rigby, P.W., Dieckmann, M., Rhodes, C. & Berg, P. Labeling deoxyribonucleic acid to high specific activity in vitro by nick translation with DNA polymerase I. *J. Mol. Biol.* **113**, 237–251 (1977).
20. Chen, Y., Wang, L., Huang, M. & Rosenberg, N. An active v-abl protein tyrosine kinase blocks immunoglobulin light-chain gene rearrangement. *Genes Dev.* **8**, 688–697 (1994).
21. Greenbaum, S., Lazorchak, A. & Zhuang, Y. Differential functions for the transcription factor E2A in positive and negative gene regulation in pre-B lymphocytes. *J. Biol. Chem.* **279**, 45028–45035 (2004).
22. Muljo, S. & Schlissel, M. A small molecule Abl kinase inhibitor induces differentiation of Abelson virus-transformed pre-B cell lines. *Nat. Immunol.* **4**, 31–37 (2003).
23. Liang, H., Hsu, L., Cado, D. & Schlissel, M. Variegated transcriptional activation of the immunoglobulin kappa locus in pre-B cells contributes to the allelic exclusion of light-chain expression. *Cell* **118**, 19–29 (2004).
24. Constantinescu, A. & Schlissel, M. Changes in locus-specific V(D)J recombinase activity induced by immunoglobulin gene products during B cell development. *J. Exp. Med.* **185**, 609–620 (1997).
25. Schlissel, M.S. & Baltimore, D. Activation of immunoglobulin κ gene rearrangement correlates with induction of germline κ gene transcription. *Cell* **58**, 1001–1007 (1989).
26. Zhong, X. & Krangel, M. Enhancer-blocking activity within the DNase I hypersensitive site 2 to 6 region between the TCR α and *Dad1* genes. *J. Immunol.* **163**, 295–300 (1999).
27. Kosak, S. *et al.* Subnuclear compartmentalization of immunoglobulin loci during lymphocyte development. *Science* **296**, 158–162 (2002).
28. Fuxa, M. *et al.* Pax5 induces V-to-DJ rearrangements and locus contraction of the immunoglobulin heavy-chain gene. *Genes Dev.* **18**, 411–422 (2004).
29. Sayegh, C., Jhunjhunwala, S., Riblet, R. & Murre, C. Visualization of looping involving the immunoglobulin heavy-chain locus in developing B cells. *Genes Dev.* **19**, 322–327 (2005).
30. Shinkai, Y. *et al.* RAG-2-deficient mice lack mature lymphocytes owing to inability to initiate V(D)J rearrangement. *Cell* **68**, 855–867 (1992).
31. Fernandez, L., Winkler, M. & Grosschedl, R. Matrix attachment region-dependent function of the immunoglobulin mu enhancer involves histone acetylation at a distance without changes in enhancer occupancy. *Mol. Cell. Biol.* **21**, 196–208 (2001).
32. Curry, J.D., Li, L. & Schlissel, M.S. Quantification of J_{κ} signal end breaks in developing B cells by blunt-end linker ligation and qPCR. *J. Immunol. Methods* **296**, 19–30 (2005).